Identification of Contact Stiffness between Brake Disc and Brake Pads Using Modal Frequency Analysis

Haizhou Ding, Qiang Zhu & Hongming Lyu*

School of Automotive Engineering, Yancheng Institute of Technology,
No. 1 Hope Avenue, Yancheng, 224051, China
*E-mail: lhmyg@163.com

Highlights:

- Contact stiffness increases with brake pressure, which leads to an increase of the mode frequency of the brake disc.
- As the disc mode order increases, the contact stiffness first increases and then almost stays invariant, which makes a mode frequency change correspondingly.
- The dependence of contact stiffness on brake pressure and disc mode order could be one of the possible reasons why the current research on prediction of brake noise and vibration is inaccurate and unsatisfactory.

Abstract. The contact stiffness between brake disc and brake pads is a vital parameter that affects brake NVH performance through increasing the system stiffness and modal frequencies. In order to establish accurate contact behavior between brake parts for further research on precise modeling of disc brakes, a method of identifying the normal contact stiffness of a floating caliper disc brake was developed in this study based on modal frequency testing and finite element analysis. The results showed that contact stiffness increases with brake pressure due to compression of the friction material and increases with the disc mode order at lower-order modes but almost stays invariant at higher-order ones due to contact area variation.

Keywords: *brake pressure; disc brake; mode frequency; mode order; normal contact stiffness; parameter identification.*

1 Introduction

Disc brakes are utilized widely in traffic vehicles and industrial machines because of the advantages of their good heat dissipation, light weight and easy maintenance. However, disc brakes sometimes produce an annoying noise or vibration while they are working. This noise or vibration may have a negative effect on perceived product quality and the surrounding environment. Because there are many sources of uncertainty in the brake system, investigating the generation mechanism of brake instability is a challenge, as is optimizing the brake system in the design stage [1-3]. Considerable research has shown that

Received October 15th, 2020, Revised March 7th, 2020, Accepted for publication July 2nd, 2020.
 ISSN: 2337-5779,
DOI: 10.5614/j.eng.technol.sci.2020.52.4.2

contact stiffness between disc and pads plays a significant role in brake dynamic behavior [4-7]. Therefore, establishing an accurate description of the contact stiffness between brake components is one of the remaining important aspects in the study of brake noise and vibration [8].

Although theoretical contact stiffness can be estimated by means of the Herz elastic contact theory [9] and the Greenwood-Williamson (G-W) statistical model [10,11], it is difficult to obtain an accurate value of contact stiffness of a real brake pair due to the uneven and time-varying contact interface. Much experimental research has been conducted on the identification of the contact stiffness of disc brakes. Júnior placed a heavy mass on a brake pad that was resting on a rigid surface and then calculated the contact stiffness between the brake pad and the rigid surface based on the measured natural frequency of the system [12,13]. Sherif identified the contact stiffness of a pad-on-disc system according to the frequency of friction-induced squeal [14]. Giannini estimated the contact stiffness from the measure of the mode split of a constrained disc [15]. Oura found that dynamic contact stiffness is independent of loading frequency but increases with load magnitude [16]. Goto, *et al*. measured the modal frequencies of a real disc brake under certain pressures and then identified the contact stiffness using finite element analysis (FEA). They concluded that contact stiffness is related to brake pressure and disc mode order. However, the authors only described the experimental process briefly and did not present the identified values of the contact stiffness [17]. It should be noted that the identified contact stiffness of a simple test apparatus may not be equal to the value of a real disc brake due to their different structures.

In order to develop a more accurate finite element model of a real disc brake assembly, a method of identifying the contact stiffness between disc and pads was investigated in this study. First, the relationship between the contact stiffness and the mode frequency of a constrained brake disc was theoretically analyzed with a two degree-of-freedom (2-DOF) model. Then, the contact stiffness of a floating caliper disc brake was identified by means of a frequency response function (FRF) and FEA. Finally, the effects of brake pressure and disc mode order on the contact stiffness was evaluated.

2 Theory of Identifying Contact Stiffness

Consider the floating caliper disc brake shown in Figure 1. When the brake pedal is pressed, brake fluid forces the piston and the right brake pad to move into contact with the disc. Then, the floating caliper moves to the right and also pushes the left brake pad against the disc through the caliper fingers. As the brake line pressure increases, the loads on both pads increase correspondingly to produce a normal force and a friction force on both sides of the rotating disc. The ability of

the contact surfaces of the brake disc and pads to resist compressive deformation due to the action of normal force is called normal contact stiffness (or contact stiffness for short in this paper).

To analyze the contact behavior of the disc brake while considering the central role of spring and mass on the system dynamics, an undamped 2-DOF lumped-parameter model was established, as shown in Figure 2, where md and mp represent the masses of the disc and the pads respectively. kd and kp are the stiffnesses of the disc and the individual pads. F is the equivalent load applied to the pad.

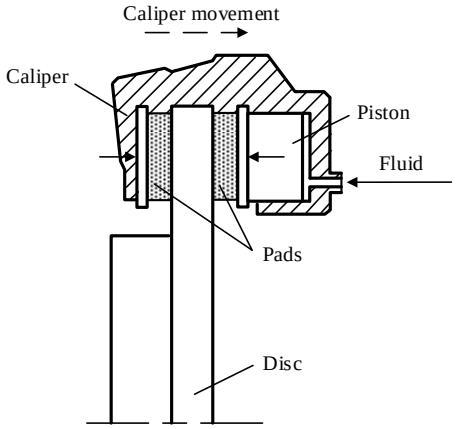

Figure 1 Schematic diagram of a floating caliper disc brake.

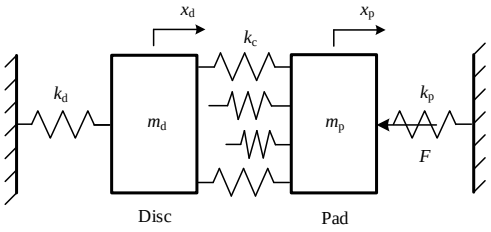

Figure 2 A 2-DOF model of a disc brake.

Considering the actual uniform contact between the brake disc and the pads, an equivalent contact stiffness kc was used to represent the overall contact behavior. The dynamic equations of this 2-DOF model were deduced as follows in Eq. (1a) and (1b) [18].

$$m_d\ddot{x}_d + k_d x_d + k_c(x_d - x_p) = 0 \tag{1a}$$

$$m_{\mathrm{p}}\ddot{x}_{\mathrm{p}} + k_{\mathrm{p}}x_{\mathrm{p}} + k_{\mathrm{c}}(x_{\mathrm{p}} - x_{\mathrm{d}}) = -F \tag{1b}$$

The eigen equation is written as in Eq. (2)

$$\begin{vmatrix} -m_{\mathrm{d}}\omega_{\mathrm{n}}^2 + k_{11} & k_{12} \\ k_{21} & -m_{\mathrm{p}}\omega_{\mathrm{n}}^2 + k_{22} \end{vmatrix} = 0 \tag{2}$$

where $k_{11} = k_{\mathrm{d}} + k_{\mathrm{c}}$, $k_{12} = k_{21} = k_{\mathrm{c}}$, $k_{22} = k_{\mathrm{p}} + k_{\mathrm{c}}$. ω_{n} is the system's eigen frequency.

The eigen frequencies of this system are solved as

$$\omega_{\mathrm{n1,2}} = \left\{ \frac{m_{\mathrm{d}}k_{22} + m_{\mathrm{p}}k_{11} \pm \left[\left(m_{\mathrm{d}}k_{22} + m_{\mathrm{p}}k_{11} \right)^2 - 4m_{\mathrm{d}}m_{\mathrm{p}} \left(k_{11}k_{22} - k_{12}^2 \right) \right]^{\frac{1}{2}}}{2m_{\mathrm{d}}m_{\mathrm{p}}} \right\}^{\frac{1}{2}} \tag{3}$$

Because the Young modulus of a disc is usually much greater than that of a brake lining, the disc stiffness k_{d} is much greater than the contact stiffness k_{c} and the disc stiffness k_{p}, i.e. $k_{11}k_{22} = (k_{\mathrm{d}} + k_{\mathrm{c}})(k_{\mathrm{p}} + k_{\mathrm{c}}) \gg k_{12}^2 = k_{\mathrm{c}}^2$. If k_{12}^2 is ignored in Eq. (3), then in Eq. (4):

$$\omega_{\mathrm{n1,2}} \approx \left[\frac{m_{\mathrm{d}}k_{22} + m_{\mathrm{p}}k_{11} \pm \left(m_{\mathrm{d}}k_{22} - m_{\mathrm{p}}k_{11} \right)}{2m_{\mathrm{d}}m_{\mathrm{p}}} \right]^{\frac{1}{2}} \tag{4}$$

Thus,

$$\omega_{\mathrm{n1}} \approx \sqrt{\frac{k_{\mathrm{d}} + k_{\mathrm{c}}}{m_{\mathrm{d}}}}, \quad \omega_{n2} \approx \sqrt{\frac{k_{\mathrm{p}} + k_{\mathrm{c}}}{m_{\mathrm{p}}}} \tag{5}$$

Eq. (5) shows that both eigen frequencies (ω_{n1}, ω_{n2}) of this system increase with the contact stiffness (k_{c}). In other words, the contact stiffness may be identified according to the variation of the natural frequency of the brake disc under different contact conditions.

3 Identification of the Contact Stiffness of a Floating Caliper Disc Brake

A real brake disc has a complex configuration while only a small part of its surface is in contact with the brake pads. If the value of contact stiffness is calculated directly from the theoretical equation in Eq. (5), a large identification

error may be generated due to model simplification. In this paper, an alternative method by using FRF and FEA is proposed to identify the contact stiffness for the floating caliper disc brake shown in Figure 3. The flow diagram of the identification procedure is illustrated in Figure 4 [19-21].

Figure 3 Photograph of the disc brake test rig.

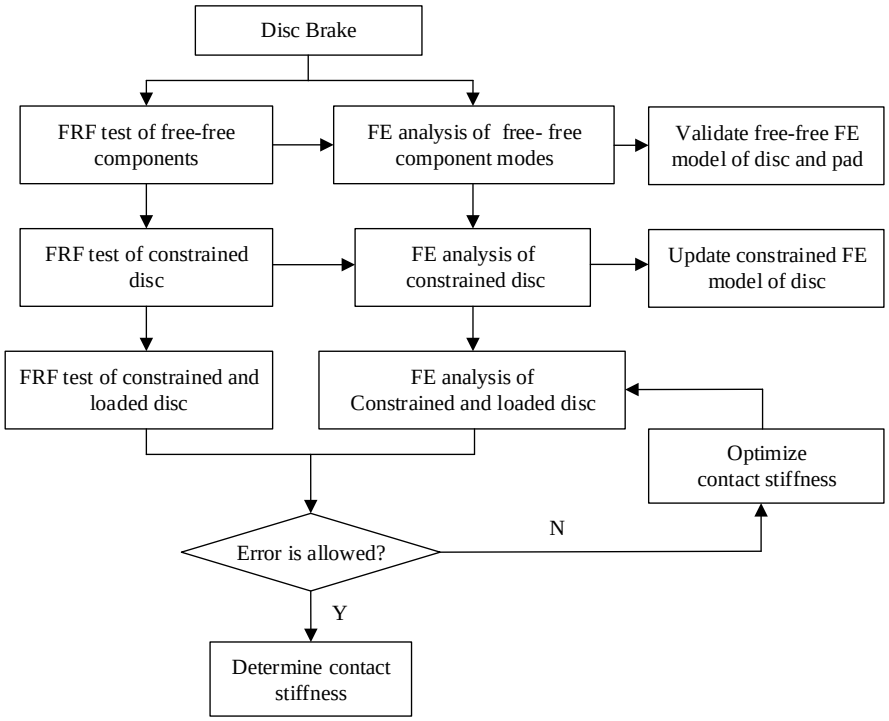

Figure 4 Flow chart for the identification of contact stiffness.

To ensure the finite element (FE) model accuracy of the disc brake, the FRF of the brake disc as well as that of the pad under free-free boundary condition was first measured by using hammer impact testing. The free-free FE models of both components were updated by setting the material property parameters to agree with the measured results. The baseline material properties of the brake disc and the pad are listed in Table 1.

Table 1 Material properties of the brake disc and pads.

Component	Material	Young's modulus (Gpa)	Poisson ratio	Density (kg/m^3)
Disc	HT150	135	0.25	7250
Back plate	Steel	206	0.26	7800
Lining	Semi-metal	10	0.35	2600

Then, the brake disc was fixed to the wheel hub through bolts on the brake test rig. The FRF of the constrained brake disc was measured by using the same hammer impact test as mentioned above. In the process of establishing the finite element model of the constrained brake disc, the bolt holes in the disc hat were set to be fully constrained in the *x*, *y* and *z* directions. Figures 5 and 6 show the simulated modal characteristics of the free-free pad and the bolted disc without brake load applied in the frequency range from 1 to 10 kHz, where (0, *i*) represents the *i*-th order out-of-plane mode of the constrained disc. The simulated results were compared with the measured modal frequencies of the physical brake components in Table 2. The good agreement between the analyzed modal frequencies and the measured data showed the validity of the FE models of the brake disc and the pad.

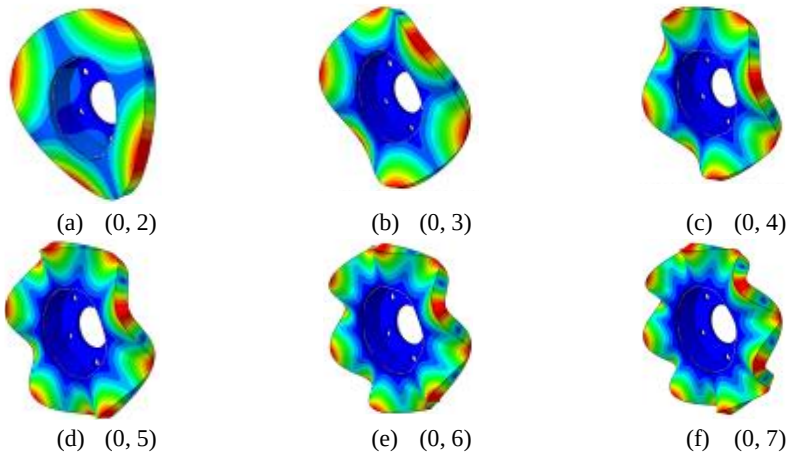

(a) (0, 2) (b) (0, 3) (c) (0, 4)

(d) (0, 5) (e) (0, 6) (f) (0, 7)

Figure 5 Mode shapes of the bolted brake disc without brake load applied (mode number in brackets).

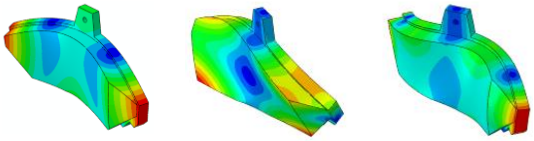

(a) 1st order (b) 2nd order (c) 3rd order

Figure 6 Free-free mode shapes of the brake pad.

Table 2 Experimental and analytical mode frequencies of the disc and the pad.

Components	Mode order	Exp. (Hz)	FEA (Hz)	Error (%)
Brake disc	(0, 2)	1227	1264	3.02
	(0, 3)	2217	2199	-0.81
	(0, 4)	3544	3522	-0.62
	(0, 5)	5223	5192	-0.59
	(0, 6)	7190	7149	-0.57
	(0, 7)	9393	9339	-0.57
Brake pad	1	2903	2898	-0.17
	2	4662	4583	-1.69
	3	6374	6675	4.72

To reduce computation time and memory consumption, a simplified FE model of an assembly only composed of a disc and a pair of pads was established using the Abaqus software. The bolt holes in the disc were still fully constrained as mentioned above, and both pads were applied with certain values of brake pressure on their back plates. Because of the physical restriction of the bracket, both brake pads were only allowed to move along the axial direction and spring constraints in the circumferential and radial directions were applied on the back plates through two reference points in the FE model. The main methods of establishing the finite element model are shown in Figure 7.

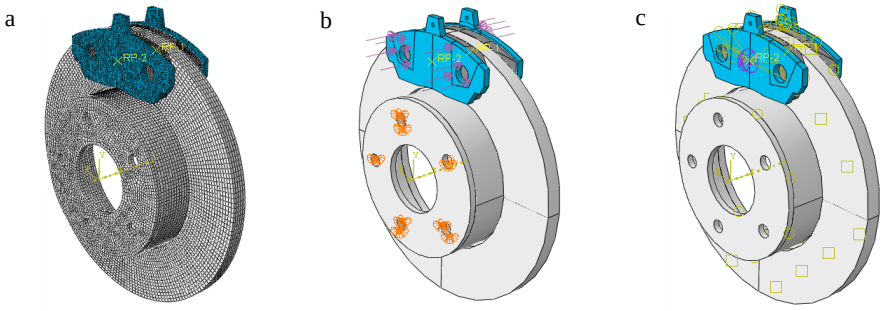

Figure 7 Simplified finite element model of the disc brake: a) meshed model, b) loading and boundary conditions and c) contact interaction and spring constraint.

When defining the contact property of interfaces, Abaqus commonly adopts a default value for normal contact stiffness based on a penalty method. This method works effectively if the material stiffness parameters are of the same order of magnitude. To avoid ill-conditioning of the global stiffness matrix and convergence difficulties, the penalty scaling factor usually ranges between 0.01 and 1. Therefore, the default contact stiffness through the penalty method is an approximate value and not an exact one.

To make the FEA results of the modal characteristics of the brake disc agree with the FRF measurement results, iterative methodologies may be used to optimize the identification of contact stiffness. Figure 8 shows the editing interface of the contact property in Abaqus. Note that the contact stiffness in this dialogue box actually represents unit area contact stiffness with N/m^3 as default unit.

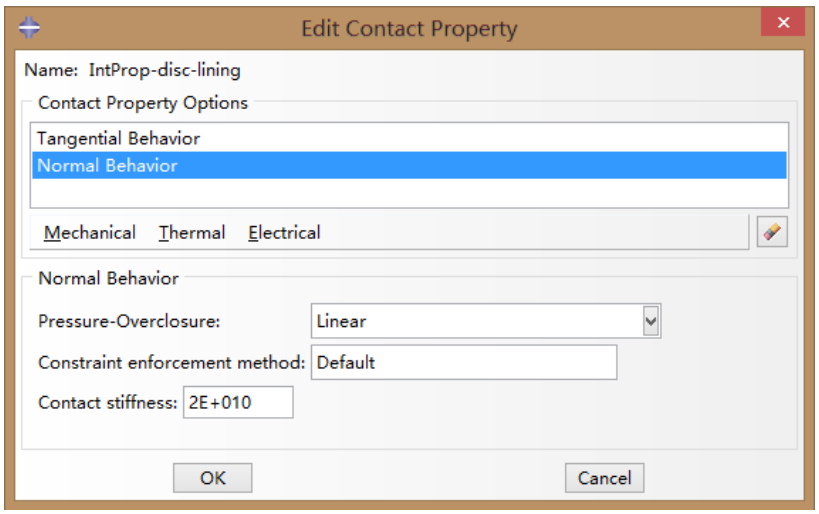

Figure 8 The definition of the contact property in Abaqus.

According to the identification procedure described above, an accelerometer was attached to the disc surface of the physical brake, as shown in Figure 3. In each test, a FRF measurement for the brake disc was performed using hammer impact testing while applying a brake load. Some of the measured FRF results of the disc under different pressures are shown in Figure 9. It can be seen that the measured 5th out-of-plane mode frequency of the constrained disc increased to 5532 Hz when the brake line pressure was set to 3 MPa, while the frequency was 5223 Hz when the pressure was zero. The corresponding contact stiffness of the brake under 3 MPa was identified as 4.73×10^{10} N/m^3 through finite element modal analysis.

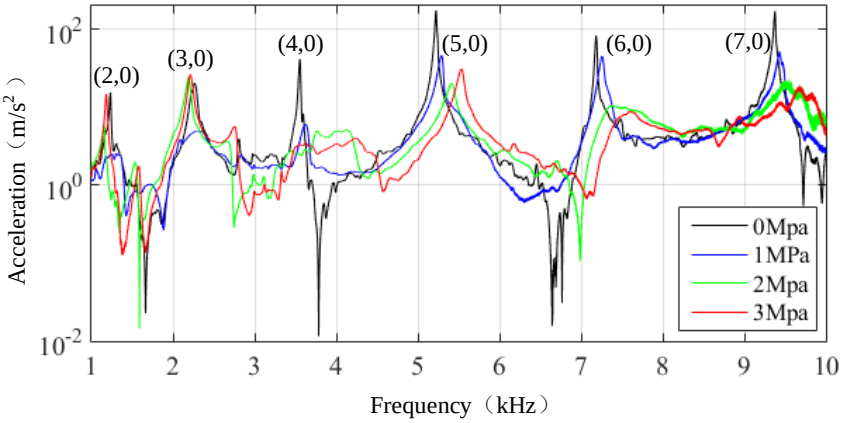

Figure 9 Frequency responses of the disc subjected to different brake line pressures.

4 Discussion of Results

Several researches have shown that contact stiffness is closely related to material properties, structural geometry and surface roughness [22, 23], etc. In this study, it was found that contact stiffness is also influenced by brake pressure and disc mode order.

4.1 Influence of Brake Line Pressure

Based on the identified results, the relationship between contact stiffness and brake line pressure was established, as shown in Figure 10. The contact stiffness shows an overall increase with brake line pressure. Considering the stress–strain relationship for friction material, Júnior assumed that contact stiffness k_c is proportional to the Young modulus E of the friction material as well as the contact area A between the pad and the disc while being inversely proportional to the thickness L of the brake lining [12], in Eq. (6):

$$k_c \propto \frac{AE}{L} \tag{6}$$

Obviously, the brake lining is more compressed when the brake pressure on the pad increases, which leads to an increase of the Young modulus of the friction material. Figure 10 also shows that when the brake pressure is lower than 3 MPa, the contact stiffness increases sharply with brake pressure due to the rapid decrease of porosity and the great increase of the Young modulus of the brake lining. However, if the brake pressure is higher than 3 MPa, the Young modulus increases slowly so that the small porosity of the brake lining decreases a little

with increasing brake pressure. Thus, the contact stiffness also increases slowly with brake pressure.

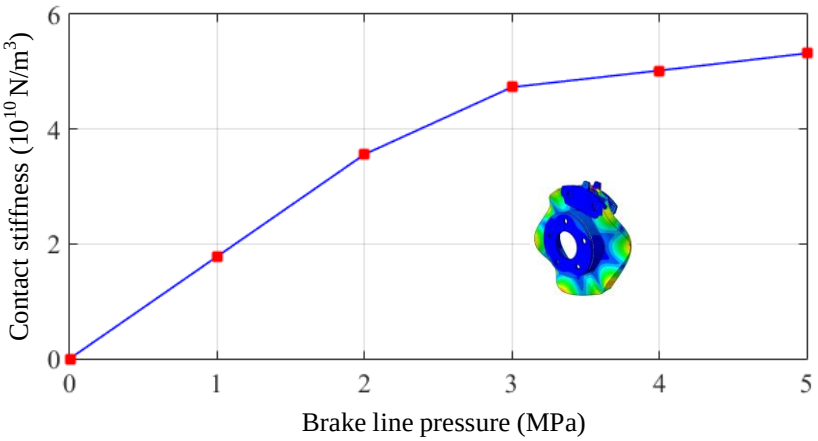

Figure 10 Contact stiffness between the brake disc and its pads versus brake line pressure.

In addition, in the process of finite element modal analysis, if the value of brake pressure on both brake pads is changed without altering the contact stiffness, the numerical results show that the disc frequency of each mode stays invariant. This means that the variation of contact stiffness is the root cause of the modal frequency shift of the brake disc.

4.2 Influence of Disc Mode Order

Because there exists damping in the brake system when brake pressure is applied, the first several disc modes are difficult to excite. By comparing the FRF curves of the brake disc under different pressures in Figure 9, it can be seen that the disc modes from the 4th to the 7th order can be excited easily if the brake pressure is set to 1 MPa. The effect of disc mode order on contact stiffness in this condition is described in Figure 11. It shows that the contact stiffness between the brake disc and pads increases with the disc mode order when the disc is in the 4th, 5th and 6th order mode. However, the contact stiffness changes little from the 6th order mode to the 7th order mode. This may be because only a small part of the disc surface is actually in contact with the brake pads when the disc is in lower order modes and more area is in contact in higher order modes. However, when the disc is in much higher order modes, the actual contact area changes little with the disc mode order, so the contact stiffness stays almost invariant.

Figure 11 also shows that the disc frequencies of lower order modes first decrease and then increase as the pressure increases. The reason is that the frequencies of

lower order modes are more likely affected by the added mass of the brake pads. For the higher modes of a brake disc, the mode frequencies are mainly influenced by the contact stiffness because the effect of the disc mode stiffness is greater than that of the added mass.

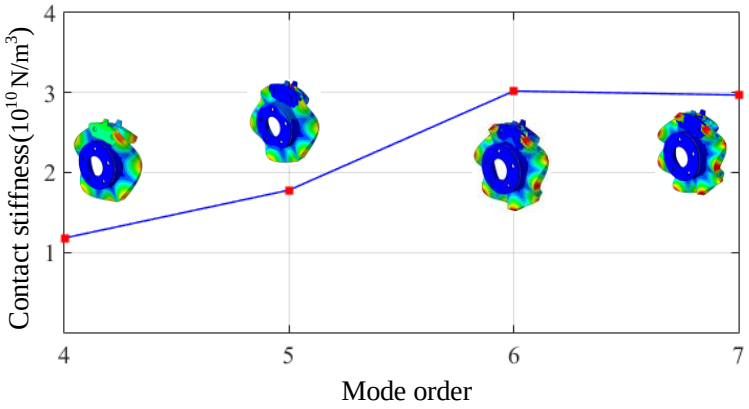

Figure 11 Contact stiffness between the brake disc and its pads versus disc mode order.

5 Conclusions

In this study, a method for identifying the contact stiffness between brake disc and brake pads was developed by using FRF and FEA. It was found that contact stiffness is closely related to brake pressure and disc mode order.

With the increase of brake pressure, the contact stiffness increases accordingly due to the porosity decrease of the brake lining, which leads to a mode frequency increase of the brake disc. As the disc mode order increases, the contact stiffness first increases and then stays almost invariant because of the variation of the contact area between the brake disc and pads, which changes the frequency of the same disc mode order correspondingly.

The dependence of the contact stiffness on brake pressure and disc mode order could be one of the possible reasons why current research on the prediction of brake noise and vibration is inaccurate and unsatisfactory. Therefore, the proposed identification method of contact stiffness may be considered for further research on disc brake modeling and simulation. However, there is also a limitation to this identification method because of the modal frequency analysis. If the brake pressure is below a certain value, the first several modes of the disc

cannot be excited and measured due to the existing system damping and thus the corresponding contact stiffness cannot be identified in such working conditions.

Acknowledgements

This work was financially supported by the National Natural Science Foundation of China (51875494), the Qing Lan Project and the Six Talent Peaks Project of Jiangsu Province (2015-ZBZZ-025).

References

[1] Lü, H., Yang, K., Shangguan, W., Yin, H. & Yu D., *Rendering Optimal Design under Various Uncertainties: A Unified Approach and Application to Brake Instability Study*, Engineering Computations, **37**(1), pp. 345-367, 2019.

[2] Zhang, Z., Oberst, S.M. & Lai, J.C.S., *Instability Analysis of Brake Squeal with Uncertain Contact Conditions*, Proceedings of 25th International Congress on Sound and Vibration (ICSV 25), Hiroshima, pp. 4031-4038, 2018.

[3] Renault, A., Massa, F., Lallemand, B. & Tison, S., *Experimental Investigations for Uncertainty Quantification in Brake Squeal Analysis*, Journal of Sound and Vibration, **367**, pp. 37-55, 2016.

[4] Abdo, J.A., *Investigation of Contact Stiffness and Its Relation to Friction-Induced Noise and Vibration*, International Journal of Modelling and Simulation, **26**(4), pp. 295-302, 2006.

[5] Fuadi, Z., Adachi, K., Ikeda, H., Naito, H. & Kato, K., *Effect of Contact Stiffness on Creep-Groan Occurrence on a Simple Caliper-Slider Experimental Model*, Tribology Letters, **33**(3), pp. 169-178, 2009.

[6] Kim, S.H. & Jang, H., *Friction and Vibration of Brake Friction Materials Reinforced with Chopped Glass Fibers*, Tribology Letters, **52**(2), pp. 341-349, 2013.

[7] Lee, M.W., Shin, M.W., Lee, W.K. & Jang, H., *The Correlation between Contact Stiffness and Stick-Slip of Brake Friction Materials*, Wear, **302**(1-2), pp. 1414-1420, 2013.

[8] Ballinger, R.A., *A Discussion of Complex Eigenvalue Analytical Methods as They Relate to the Prediction of Brake Noise*, SAE International Journal of Passenger Cars – Mechanical Systems, **9**(1), pp. 183-198, 2016.

[9] Hertz, H., *On the Contact of Elastic Solids*, Journal fur die Reine und Angewandte Mathematik, **92**, pp. 156-171, 1882.

[10] Greenwood J.A. & Williamson J.B.P., *Contact of Nominally Flat Surfaces*, Proceedings of the Royal Society A Mathematical Physical and Engineering Sciences, **295**(1442), pp. 300-319, 1966.

[11] Greenwood, J.A. & Williamson, J.B.P., *Developments in the Theory of Surface Roughness*, Proceedings of the 4th Leeds-Lyon Symposium on Tribology, Lyon, pp. 167-177, 1977.
[12] Júnior, M.T., Gerges, S.N.Y. & Jordan, R., *Analysis of Brake Squeal Noise Using the Finite Element Method: A Parametric Study*, Applied Acoustics, **69**(2), pp. 147-162, 2008.
[13] Júnior, M.T., Gerges, S.N.Y. & Cordioli, J., *Analysis of Brake Squeal Noise Using FEM Part I: Determination of Contact Stiffness between Rotor and Pads*, SAE Technical Paper 2004-01-3330, 2004.
[14] Sherif, H., Blouet, J., Cretegny, J., Gras, R. & Vialard, G., *Experimental Investigation of Self-excited Squeal*, SAE Technical Paper 892451, 1989.
[15] Giannini, O., & Sestieri, A., *Predictive Model of Squeal Noise Occurring on a Laboratory Brake*, Journal of Sound and Vibration, **296**(3), pp. 583-601, 2006.
[16] Oura, Y., Kurita, Y., Nishizawa, Y. & Kosaka, K., *Comparison of Pad Stiffness under Static Pressure and Vibration with Small Amplitude*, SAE Technical Paper 2012-01-1818, 2012.
[17] Goto, Y., Amago, T., Chiku, K., Matsushima, T. & Ishihara, T., *Experimental Identification Method for Interface Contact Stiffness of FE Model for Brake Squeal*, Proceedings of the IMechE Conference on Braking 2004: Vehicle Braking and Chassis Control, London, pp. 143-155, 2004.
[18] Sinha, A., *Vibration of Mechanical Systems*, Cambridge University Press, New York, USA, 2010.
[19] Tonazzi, D., Massi, F., Salipante, M., Baillet, L. & Berthier, Y., *Estimation of the Normal Contact Stiffness for Frictional Interface in Sticking and Sliding Conditions*, Lubricants, **7**(7), p. 56, 2019. DOI: 10.3390/lubricants 7070056.
[20] Zheng, Y., Hou, Z. & Rong, Y., *The study of Fixture Stiffness – Part II: Contact Stiffness Identification between Fixture Components*, International Journal of Advanced Manufacturing Technology, **38**(1-2), pp. 19-31, 2008.
[21] Zhao, G., Xiong, Z., Jin, X., Hou, L. & Gao, W., *Prediction of Contact Stiffness in Bolted Interface with Natural Frequency Experiment and FE Analysis*, Tribology International, **127**, pp. 157-164, 2018.
[22] Sherif, H.A., *Parameters Affecting Contact Stiffness of Nominally Flat Surfaces*, Wear, **145**(1), pp. 113-121, 1991.
[23] Pharr, G.M., Oliver, W.C. & Brotzen, F.R., *On the Generality of the Relationship Among Contact Stiffness, Contact Area, and Elastic Modulus during Indentation*, Journal of Materials Research, **7**(3), pp. 613-617, 1992.